Original Article

Computational investigation of structural, spectral, electronic, and pharmacological properties of 4-trifluoromethyl phenyl thiourea and 4-trifluoromethyl phenyl isothiocyanate: insights into nonlinear optical and anticancer potentials

S.N.Saravanamoorthy [1]

1. Department of Physics, Devanga Arts College, Aruppukottai.

Email Id: snsaravanamoorthy@gmail.com

Abstract

The structural, spectral, thermodynamic, and electronic properties of the two investigated compounds, 4-Trifluoromethyl Phenyl Thiourea (4TFMPTU) and 4-Trifluoromethyl Phenyl Isothiocyanate (4TFMPIC), have been systematically analyzed using computational approach. The optimized molecular geometries confirm the stability and reliability of the calculated bond lengths and bond angles, which align closely with experimental and previously reported values. Spectral investigations, including IR and UV-Vis analyses, further reinforce the presence of functional groups and confirm the vibrational characteristics associated with the C-H, C-N, C-F, and C=S bonds. The UV spectra reveal significant electronic transitions ($n \rightarrow \pi^*$ and $\pi \rightarrow \pi^*$), indicating the compounds' optical activity and potential applications in photonics and optoelectronics. Mulliken atomic charges and Molecular Electrostatic Potential (MEP) maps offer a detailed understanding of electron distribution and reactive sites. The lower energy gap of 4TFMPTU (2.12 eV) suggests greater chemical reactivity and potential utility in various chemical and biological processes. The higher global softness and electrophilicity index values also indicate that 4TFMPTU is more susceptible to electronic transitions, making it a versatile molecule for further functionalization. Polarizability and hyperpolarizability assessments indicate strong nonlinear optical (NLO) properties, particularly for 4TFMPIC, which exhibits a β value 7.95 times higher than that of urea. These findings highlight its potential in optical applications, such as sensors, switches, and other photonic devices. The docking analysis revealed strong binding affinities of both compounds with multiple target proteins, emphasizing 4TFMPTU as a highly potent breast cancer inhibitor with a binding affinity of -6.0 kcal/mol and several stabilizing interactions. Similarly, 4TFMPIC demonstrated notable binding efficacy, exhibiting a binding affinity of -5.7 kcal/mol. Both compounds displayed low excretion rates, indicating prolonged retention in the body, which may enhance their therapeutic potential. Furthermore, their role as substrates for CYP1A2 suggests improved bioavailability by reducing metabolic degradation. Both 4TFMPTU and 4TFMPIC demonstrate considerable promise as potential drug candidates, particularly for addressing breast cancer.

Keywords

Molecular Docking, Nonlinear Optical Properties, 4-Trifluoromethyl Phenyl Derivatives, Breast Cancer Inhibition

Introduction

Investigating the molecular docking study of 4-Trifluoromethyl Phenyl Thiourea (4TFMPTU) and 4-Trifluoromethyl Phenyl Isothiocyanate (4TFMPIC) on diverse proteins is of significant interest, as isothiocyanates (ITCs) are naturally occurring defensive compounds found in various cabbage-related crop plants. ITCs have attracted interest due to their antimicrobial and anticancer effects [1]. In medicine, their potential as anticarcinogenic agents [2,3] and antimicrobials has been explored, with implications for novel antibiotic design [4,5]. In addition, ITCs are being explored for use in biofumigation for crop protection. Notably, Broccoli sprouts, a nutrient-rich vegetable, contain chemical compound families, including ITCs, known for their chemopreventive properties [6,7,8]. ITCs derived from broccoli sprouts have been specifically investigated for their health benefits, including anticancer and antioxidant effects, as well as their ability to activate phase 2 detoxifying enzymes [9]. Many studies have assessed the antioxidant capabilities of ITCs in different natural products [10], suggesting that their antioxidant potency may differ based on the type of functional groups or the quantity of methylene groups in the side chain [11]. Recent findings show that a single crystal of the small molecule 4TFMPIC undergoes plastic deformation when bent, twisted, or coiled. The unique feature of 4TFMPIC has been leveraged in the creation of a piezoresistive composite sensor [12]. Thioureas, compounds composed of sulfur and nitrogen, have gained significance in drug research.Acyl thiourea derivatives are of interest to scientists for their diverse applications, such as combating viruses, bacteria, and fungi, and targeting ailments such as HIV, cancer, and inflammation [13]. Furthermore, thioureas can be used to manage plant pathogens such as Penicillium expansum (PE) and Fusarium oxysporum (FO) [14].Data on the biological activity of 4TFMPTU and 4TFMPIC derivatives against breast cancer is scanty. Despite the wealth of information on the beneficial properties of isothiocyanate and thiourea based compounds, there is currently no evidence exploring the in silico profiling of 4TFMPTU and 4TFMPIC through a comprehensive molecular docking study on diverse proteins particularly hormone signaling in breast cancer. This gap in knowledge underscores the need for further research to gain insights into the potential antioxidant mechanisms of these compounds.

MATERIALS AND METHODS

The structures of 4-Trifluoromethyl Phenyl Thiourea (4TFMPTU) and 4-Trifluoromethyl Phenyl Isothiocyanate (4TFMPIC) are downloaded from the PubChem website. Quantum chemical calculations were performed on the molecule 4TFMPTU and 4TFMPIC using the Gaussian 09W program. The calculations used a specific method (DFT) and a basis set (6-311+G) to understand the molecule's properties. The molecular structure was optimized to find its most stable shape. Then, the vibrational spectra were calculated and interpreted using a special analysis (PED). A visualization program (Gauss View 05) was used to animate the molecule's vibrations and

verify their accuracy. The electronic absorption spectra were predicted using another method (TD-DFT). The molecule's energy levels were analyzed, including the HOMO-LUMO gap. The density of states spectrum was simulated using a special program (Gauss Sum 3.0). Several energy parameters were calculated, including ionization energy, electron affinity, and electronegativity. Additional analyses were performed, including natural bond orbital (NBO) analysis and molecular electrostatic potential (MEP) surface mapping.

We got the 3D structures of proteins from the Protein Data Bank (PDB), a database managed by the Research Collaboratory for Structural Bioinformatics. We used a computer program called AutoDock Vina to see how our two compounds fit onto different proteins. This helped us find the exact spots where they bind and how strongly they bind. Before running the docking analysis, we prepared the proteins and compounds for docking using a program called AutoDock Tools (ADT). We created files and set up the grid box for the analysis. After docking, we took the best pose (the one with the lowest energy) and aligned it with the protein structure. We then visualized the results using a program called PyMOL2 to learn more about how the compounds bind to the proteins.

RESULT AND DISCUSSION

STRUCTURAL ANALYSIS

The structures of the title compounds are optimized and its structures are displayed in Figure 1. The thiourea and isothiocyanate system are linked to the trifluoromethyl phenyl group through bond distances C12=N5 and C5-N4, measuring 1.41 and 1.39 Å, respectively. The experimentally determined bond distance connecting the trifluoromethyl phenyl group to the other system, reported as 1.4 Å, precisely aligns with the values documented in previous literature [15,16]. Within the molecules under examination, the bond distances of F2-C9 in 4TFMPIC and C11-F12 in 4TFMPTU are both reasonable, each measuring 1.39 Å. The bond distances within the phenyl ring of our investigated molecules are 1.39 Å for Carbon-Carbon bonds and 1.08 Å for Carbon-Hydrogen bonds. Our calculations of bond distances within the N=C=S group align with the findings reported by Dahinel I et al. in their study [17]. Specifically, in the N=C=S group, the bond distance for C13=N5 is 1.18 Å, and for C13=S1, it is 1.59 Å. Typical bond angles for N5-C13-S1 and C12-N5-C10 linkages in isothiocyanate are 178° and 120° respectively. N-C-S diverges slightly from 180°.

Thiourea's nitrogen, oxygen, and sulfur atoms serve as donor atoms, contributing electrons to create bonds and offering diverse bonding possibilities. The molecule 4TFMPTU exhibits both intra and intermolecular hydrogen bonding, involving N-H proton-donor groups and predominantly sulfur atoms. The presence of the C=S group within the same molecule makes it particularly interesting for further investigation. The bond distances for N4-H17, N4=C2, C2-S3, and C2=N1 in the thiourea group are calculated to be 1.01, 1.37, 1.66, and 1.36 Å, respectively. These calculated values closely match those obtained through previous experimental methods [18,19]. The bond lengths of N1-H15 and N1-H16 within the NH2 group measure 1.01 Å. The trifluoromethyl phenyl group and the thiourea

group are linked through the N4-C5-C6 bond angle, which measures 124°. The bond angles for N1-C2-N4 and N1-C2-S3 are 111° and 117°, respectively.

Spectral Investigations

IR INVESTIGATION OF 4TFMPIC:

Several stretching vibrations for various groups like C-H, C-N, C-F, C-C and NCS have been documented in previous literature [20-24]. The information from the preceding literature proves beneficial in confirming the presence of various functional groups in our molecule, 4TFMPIC. Figure 2 shows the theoretically computed IR Spectra of 4TFMPIC. In the case of 4TFMPIC, two symmetric and two asymmetric C-H stretching vibrations are observed around 3200 cm-1, with an approximate potential energy distribution value of 86%. Notably, the typical C-H stretching frequency in phenyl usually falls within the range of 3000 cm-1 to 3100 cm-1. Silverstein and his team explored C-N stretching absorption in the spectral range of 1382-1266 cm-1. Identifying the C-N stretching frequency can be challenging due to potential confusion with other vibrations. In this study, a band at 1305 cm-1 is confirmed to be associated with C-N stretching vibrations, with a potential energy distribution (PED) value of 74%. The stretching movements of C-F bonds are commonly observed between 1100 and 1200 cm-1. The band at 1134 cm-1, with a PED of 78%, is identified as the symmetric stretching vibration in IR spectra.

In the spectral range of 1625-1430 cm-1, the stretching vibrations of C-C bonds in the ring are observable. For aromatic six-membered rings like benzene and pyridines, multiple bands emerge due to skeletal vibrations, with the most intense typically occurring around 1500 cm-1. Interestingly, in our specific molecule, 4TFMPIC, the most prominent band is observed at 1580 cm-1. Concerning isothiocyanates, the doubly degenerate bending mode of the NCS moiety is noted at approximately 470 cm-1, while the theoretically expected NCS bend mode is calculated to appear at 431 cm-1. The C=S group is linked to the nitrogen element. CNR Rao and Venkataraghavan assigned the C=S stretching frequency to the region of 1225 – 1025 cm-1. In our prediction, the stretching frequency of the C=S band occurs at 980 cm-1.

IR INVESTIGATION OF 4TFMPTU:

Figure 3 represents the theoretically computed IR Spectra of 4TFMPTU. In the study by B. Ravi et al. [25], the NH2 stretching vibrations of thiourea single crystals were reported to occur around 3300 cm-1. In our current investigation, the N-H symmetry stretching vibration is detected at 3558 cm-1, while the asymmetry NH vibration is observed at 3680 cm-1, with a noteworthy potential energy distribution (PED) of 95%. For 4TFMPTU, the symmetric C-H stretching vibration manifests at 3185 cm-1, with a high potential energy distribution value of 97%. The C-N stretching absorption is explored at 1315 cm-1 in the IR spectral profile. C-F bond stretching movements, commonly observed between 1100 and 1200 cm-1, reveal an asymmetric band at 1130 cm-1, identified with a PED of 69. The ring C-C stretching vibration spans the region from 1625 to 1430 cm-1, often intertwining with CH and OH bending vibrations. The carbon-carbon asymmetry stretching mode appears at 1349 cm-1, while the carbon-carbon

symmetry stretching mode is noted at 1680 cm-1. Thiourea exhibits a distinctive C-S symmetry stretching vibration, evident in its spectral behavior at 703 cm-1. In Mahendra Kumar Trivedi's previous research, alterations in the N-C-S bending peak frequency, specifically from 621 to 660 cm-1, were observed in treated thiourea. This change suggests potential modifications in the bond angle following biofield treatment [26]. In our IR profile, the bending vibration of the N-C-S peak is evident at 425 cm-1.

UV SPECTRAL STUDY

The optical transmission spectrum provides important details about the molecule's structure. It absorbs UV and visible light, causing electrons to move from lower to higher energy states in σ and π orbitals. The UV spectra for 4TFMPIC and 4TFMPTU are shown in Figure 4. The maximum absorption peak in the UV spectra of 4TFMPIC molecule was detected at 252nm with oscillator strength of 0.0102. n-Electrons are unattached electrons in atoms like N, O, halogens, and S. They're not as tightly held as σ-electrons. In this situation, ultraviolet and visible energy can trigger the excitation process. For the 4TFMPIC molecule, the UV peak occurs at 252 nm, falling within the expected range for $n \rightarrow \pi^*$ transitions. According to a study by G. Madhurambal and colleagues, the bonding π and antibonding π^* absorption band is observed for urea at 236 nm and for thiourea at 255 nm [27]. Thiourea (CH_4N_2S) is a compound that contains sulfur and nitrogen atoms, and its crystal structure can exhibit interesting characteristics when exposed to UV light. B. Ravi and his team noted a strong absorption range of 190 to 300 nm in the absorption spectrum of the thiourea crystal [28]. Also, UV spectroscopic analysis of 4TFMPTU molecule showed maximum absorption at 378nm and caused by electronic transitions from $\pi \rightarrow \pi^*$ with oscillator strength of 0.014. The absorptions are broad because the electronic transitions overlap with other molecular energy states. According to C.Raveendiran et. al., the basic necessity and advantage for a material having NLO properties are the nonexistence of absorption in the constituency 350-1100 nm [29]. The energy values of 4TFMPIC and 4TFMPTU were lying at an energy value of 4.92 eV and 3.28 eV respectively.

THERMODYNAMIC PROPERTIES

Thermochemical analysis is conducted at a standard room temperature of 298.15 K and 1 atmospheric pressure, with various calculated thermodynamic parameters presented in Table 1. SCF energy represents that the electronic structure is consistent with the calculated molecular orbitals. Lower SCF energy indicates that greater stability. Total energy predicts the key properties including reaction pathways and spectroscopic features and also it provides essential insights into the behaviour and stability of the molecules [30]. Based on our calculation both molecules show that greater stability. A molecule's dipole moment, reflecting its polarity, can influence interactions with biological systems and impact its biological activity. The dipole moment value for 4TFMPIC and 4TFMPTU is 1.54 and 7.2815 Debye respectively. Molecules with low dipole moments in 4TFMPIC exhibit less polarity and are often nonpolar in nature. The entropy at room temperature

is determined as 117.097 cal mol−1 K−1 for 4TFMPTU and 105.735 cal mol−1 K−1 for 4TFMPIC. Comprehending heat capacity is essential for predicting how molecules store and release energy, thereby influencing a range of chemical and physical processes. A lower heat capacity 38.57 cal mol−1 K−1 for 4TFMPIC is considered more favourable, indicating that the substance requires less heat to change its temperature.

Table 1: The calculated thermodynamic parameters of our studied molecules

Thermodynamic parameters (298K)	4TFMPTU	4TFMPIC
Self-Consistent Field (SCF) energy (a.u)	-1116.10	-1059.54
Total energy in kcal mol^{-1}	101.140	73.224
Heat capacity at const. volume, Cv (cal mol^{-1} K^{-1})	47.01	38.57
Entropy, *S* (cal mol^{-1} K^{-1})	117.097	105.735
Vibrational energy, Evib (kcal mol^{-1})	99.362	71.447
Zero-point vibrational energy, E0 (kcal mol^{-1})	93.19	66.69
Rotational constants (GHz)		
A	1.67352	2.73520
B	0.24109	0.23189
C	0.21935	0.22263
Dipole Moment (Debye)	7.2815	1.54

MULLIKEN ATOMIC CHARGES

Mulliken atomic charges serve as crucial descriptors in quantum chemistry, offering insights into the distribution of electrons within molecules. In our study, we employed the DFT/B3LYP method to calculate Mulliken atomic charges for two title compounds, namely 4TFMPTU and 4TFMPIC. These charges are graphically depicted in the accompanying figure 5, revealing intriguing patterns within the molecular structures. Remarkably, our results unveil a consistent trend across both compounds, with all hydrogen atoms exhibiting positive charges. However, a notable disparity emerges between the hydrogen atoms of the two compounds, particularly highlighted by the highly positive charge of H15 in 4TFMPTU (0.359), in contrast to the hydrogen atom in 4TFMPIC. This discrepancy can be attributed to the distinct chemical environment surrounding H15, as it is bonded to the most electronegative nitrogen atom (N1) within the 4TFMPTU molecule.

Further examination of the nitrogen atoms within the compounds sheds additional light on their charge distribution. Notably, nitrogen atom N1 in both compounds exhibits a highly negative charge, with a value of -0.718. This observation highlights the significant electronegativity of nitrogen in these molecules. Conversely, another nitrogen atom, N4, displays a slightly lower negative charge of -0.777, indicating a lesser degree of electron withdrawal compared to N1. Moreover, our analysis reveals intriguing insights into carbon atom C9 within 4TFMPIC. This particular carbon atom manifests a notably higher charge, which can be attributed to its bonding configuration with three electronegative fluorine atoms. Such interactions result in a greater electron deficiency on carbon, contributing to its elevated Mulliken atomic charge. In summary, our investigation into Mulliken

atomic charges elucidates intricate electronic properties within the studied compounds, providing valuable information for understanding their chemical reactivity and structural characteristics.

MOLECULAR ELECTROSTATIC POTENTIAL (MEP) ANALYSIS

Examining the electrostatic potential map, depicted in Fig 6., proves crucial for exploring the molecular attributes and intermolecular associations that significantly influence the binding of a substrate to its reactivity centers. These maps unveil regions exhibiting the highest probability for positive and negative charge interactions on the examined carbon-based compound. By assessing the most negative and positive values of the MEP, valuable insights into the electron-donating and accepting tendencies of a specific molecule are gleaned. To identify potential sites for positive and negative charge interactions in 4TFMPIC and 4TFMPTU, MEP calculations were conducted using the B3 Exchange-correlation approach with an appropriate basis set.

Within Gauss View, the 3D map color code for the Molecular Electrostatic Potential (MEP) in 4TFMPIC spans from -3.396 atomic units (a.u.) to +3.396 a.u. In the instance of 4TFMPIC, the most conspicuous negative electrostatic potential is localized at the CF3 group. These areas denote favorable sites for electrophilic attacks, exhibiting values ranging from -0.014 a.u. to -0.024 a.u. The maximum positive electrostatic potential (0.03 a.u.) corresponds to hydrogen atoms H14 to H17 within the phenyl group.

Within the 4TFMPTU substance, the color spectrum of the Molecular Electrostatic Potential (MEP) extends from -8.131 x 10-2 (intense red) to +8.131 x 10-2 (intense blue). Particularly noteworthy is the prime area for nucleophilic reactions, located on the NH2 and NH in the thiourea group. Clear indications of electrophilic regions are observed around the three fluorine atoms in the CF3 group, representing pivotal sites for both positive and negative charge attractions. These discoveries provide valuable insights into molecular interactions, facilitating inquiries into bioactivity.

FMOS STUDY

Frontier Molecular Orbitals (FMOs) are crucial in molecular interactions and offer key insights into the optical, electronic, and reactivity aspects of the studied molecule. The least energy gap value is found to be 2.12 eV for 4TFMPTU while highest energy gap value 5.75 eV is observed for 4TFMPIC molecule. The highest ionization potential (IP) is 7.55 in 4TFMPIC, whereas the lowest is 5.28 in 4TFMPTU. In 4TFMPTU, the highest electron affinity (EA) is 3.16, while in 4TFMPIC, the least value is 1.8. Comparatively, IP values indicate a greater electron-donating capability in the studied molecules, as IP values are generally larger than EA values[31,32]. Usually high Eg value is indicating non-reactivity and stability. In our study we found lowest energy gap of 2.12 eV for 4TFMPTU molecule. Global hardness is found using the formula Hardness (η) = (EHOMO - ELUMO)/2. The value of η (1.06) is found to be for 4TFMPTU molecule. In FMO studies, the energy gap (Eg) of a molecule is inversely related to its global hardness. From this, we can infer that the global hardness value is relatively small when

compared to the energy gap values observed in our two studied molecules. Understanding global softness (S) helps predict a molecule's behavior in various environments and reactions [33]. The high value of global softness (0.943) in 4TFMPTU molecule indicates greater susceptibility to electronic changes and potential for diverse chemical interactions. Electrophilicity index (ω) gauges the electron-accepting capacity and is measured by using $\omega = \mu\ 2/2\eta$ [34]. Here μ is termed as the electronic chemical potential. The 4TFMPTU molecule registers a value of 8.39 on the higher end, whereas the 4TFMPIC molecule records a lower value of 3.79. Both ω and μ tells the propensity for engaging in electron transfer reactions. The energy of back donation (Eb-d) helps us understand how strong the interaction is between donor and acceptor orbitals. This interaction affects things like bond strength, catalytic activity, and how the molecule behaves overall. It can be obtained by the formula Eb-d = -η/4. The back donation is stronger in the 4TFMPIC compound with a value of -0.717 compared to the -0.265 value in the 4TFMPTU compound.

POLARIZABILITY

Calculations show that two compounds, 4TFMPIC and 4TFMPTU, have dipole moments of 1.541 and 7.2815 Debye. The 4TFMPTU compound has the highest dipole moment. Both compounds have similar mean polarizability values, but they're negative. This might mean they have high hyperpolarizability, which is important for nonlinear optical (NLO) properties. To confirm, we calculated the hyperpolarizability (β) values. The β values for 4TFMPIC and 4TFMPTU are 1.511 × 10-30 esu and 1.070 × 10-30 esu. For comparison, urea (a common reference molecule) has a β value of 0.1947 × 10-30 esu [35]. The 4TFMPIC compound's β value is 7.95 times higher than urea's. This suggests that 4TFMPIC is a good NLO material. A high β value indicates efficient charge movement and strong NLO response, making it useful for applications like optical switches and sensors.

Table 2: Dipole moments, static electronic polarizabilities, first-order hyperpolarizabilities and second-order hyperpolarizabilities

	4TFMPIC **Debye**	4TFMPTU **Debye**		4TFMPIC **(a.u.)**	4TFMPTU **(a.u.)**		4TFMPIC **(a.u.)**	4TFMPTU **(a.u.)**
μ_x	1.3595	-4.1613	β_{xxx}	129.60	-78.83	γ_{xxxx}	-5455.52	-4175.08
μ_y	0.0137	5.9751	β_{xxy}	1.3166	88.69	γ_{yyyy}	-361.48	-628.17
μ_z	-0.726	-0.0501	β_{xyy}	23.9973	8.559	γ_{zzzz}	-149.94	-160.71
μ_{total}	1.541	7.2815	β_{yyy}	-1.6685	26.557	γ_{xxyy}	-149.94	-833.12
α_{xx}	-108.91	-89.05	β_{xxz}	-0.0218	0.775	γ_{xxzz}	-849.73	-838.11
α_{yy}	-72.32	-77.95	β_{xyz}	-0.0006	-0.214	γ_{yyzz}	-96.83	-153.42
α_{zz}	-82.13	-91.86	β_{yyz}	0.0118	1.935	$\langle\gamma\rangle$	-1631.988	-1722.652
α_{xy}	0.3087	-19.39	β_{xzz}	21.3248	23.676			
α_{xz}	-0.0014	-0.809	β_{yzz}	1.6581	-0.453			
α_{yz}	0.0001	0.143	β_{zzz}	-0.0029	-1.022			
α^{iso}	-87.786	-86.286	β_{tot}	174.92	123.90			
$\Delta\alpha$	-31.685	-4.145	β_{μ}	135.47	120.82			
η_{α}	-0.464	-5.025						

MOLECULAR DOCKING

DRUG-LIKENESS PROPERTIES

Lipinski's Rule of Five (LRoF) helps evaluate whether a compound is likely

to be a good drug based on its molecular weight, fat solubility, and the number of hydrogen bond donors and acceptors [36]. It is widely used in medicinal chemistry to select compounds that are more likely to be safe and effective drugs. Unlike Lipinski's rules, Veber's rules focus specifically on factors that affect how well a drug can be absorbed when taken orally. Table 3 shows that none of the compounds we studied broke more than one rule from Lipinski or Veber. This is generally acceptable, but further evaluation is still necessary. Compounds with LogBB values less than 0.3 and LogPS values less than -2 are considered unable to cross the Blood-Brain Barrier (BBB) and enter the Central Nervous System [37]. For 4TFMPTU, the LogPS and LogBB values are -1.95 and 0.30, respectively, while for 4TFMPIC, they are -1.94 and 0.34. Based on distribution predictions, 4TFMPTU seems more suitable for drug development than 4TFMPIC.

We also analyzed how the liver processes and removes these compounds by measuring total clearance. A lower clearance value means the drug stays stable in the body for longer (Pires et al., 2015). The total clearance for 4TFMPTU is -0.188, while for 4TFMPIC, it is 0.181. These low clearance values suggest the compounds may remain in the body for a longer time, potentially improving their effectiveness. In terms of metabolism, both compounds act as substrates for CYP1A2 enzymes. Inhibiting this enzyme can slow down metabolism, increasing the bioavailability and prolonging the effects of the compounds in the body. We also assessed how easy it is to synthesize these compounds, which is important for practical testing. The synthetic acceptability (SA) score ranges from 0 to 10, where a value closer to 1 means the compound is easy to produce [38]. The SA values for these compounds range between 1.45 and 1.77, indicating they are relatively simple to synthesize.

Table 3: Drug-like properties profile based on Lipinski and Veber Rule for the proposed compounds

Property profile	Expected range	4TFMPIC	4TFMPTU
MW	< 500	203.18	220.21
Log P	≤ 5	2.36	1.90
nHBA	< 10	4	3
nHBD	≤ 5	0	2
TPSA	< 140	44.45	70.14
nRotB	<10	2	3

MW- Molecular weight in Dalton; LogP - Logarithm of partition coefficient of the compound between n-octanol and water; nHBA - Num. H-bond acceptors; nHBD - Num. H-bond donors; TPSA - Topological Polar Surface Area in Å2; nRotB - Num. rotatable bonds.

DOCKING ANALYSIS WITH AUTO DOCK VINA

We used molecular docking analysis with AutoDock Vina to predict where our two compounds bind to different proteins. This analysis helped identify binding sites and measure binding strength based on binding affinity values. Protein and ligand files were prepared using AutoDock Tools (ADT), and results were visualized with PyMOL2. Protein structures were retrieved from the Protein Data Bank (PDB). Key examples include PDB ID 5NQR, which targets hormone signaling in breast cancer, and PDB ID 8HOK, involved in biochemical processes. Other proteins studied include RNA

repair enzymes, metabolic regulators, and SARS-CoV-2 spike proteins. Table 4 lists the binding affinity values and hydrogen bond distances, while Figures 7 and 8 show 2D and 3D views of the interactions. Docking results showed binding energies between -5.0 and -6.0 kcal/mol, suggesting strong binding potential. The compound 4TFMPTU had a binding affinity of -6.0 kcal/mol, forming a hydrogen bond with SER137A and pi-cation interactions with ARG51A, improving stability. It also formed halogen bonds with GLU93A, enhancing molecular recognition. The compound 4TFMPIC showed a binding affinity of -5.7 kcal/mol and formed a hydrogen bond with GLU93A, indicating its potential as a breast cancer inhibitor. Further studies examined interactions with additional proteins. For example, 4TFMPTU bound to protein 8HOK with a -6.0 kcal/mol affinity, forming a hydrogen bond with SER130A, and to protein 8BTT with -5.8 kcal/mol affinity, forming stable hydrogen bonds. Similarly, 4TFMPIC had affinities of -5.6 and -5.5 kcal/mol with proteins 8HOK and 8BTT. Both compounds also showed pi-stacking interactions, improving stability and precision. Protein 7YD0 showed the lowest binding energy (-5.0 kcal/mol), forming hydrogen bonds with GLN957B and SER316A. These results highlight 4TFMPTU and 4TFMPIC as promising candidates for drug design. Further studies will explore their mechanisms and improve their bioactivity.

Table 4: Analyzed binding energy values, the residues involved, and their interaction distances

PDB ID	Binding affinity value of 4TFMPIC				Binding affinity value of 4TFMPTU			
	BA	Res	D(H-A)	D(D-A)	BA	Res	D(H-A)	D(D-A)
5NQR	-5.7	GLU 93A	3.1	3.8	-6.0	SER 137A	2.3	3.1
8HOK	-5.6	SER 130A	2.2	2.3	-6.0	SER 130A	2.1	2.98
8BTT	-5.5	ASN 354A	2.6	3.02	-5.8	ASN 354A	2.4	2.9
8V5G	-5.3	TRP 334B	2.6	3.07	-5.7	THR 381B	2.3	3.0
8BS5	-5.2	THR 535A	2.4	3.24	-5.1	TYR 424A	2.6	3.1
7YD0	-5.1	GLN 957B	2.6	3.25	-5.0	SER 316A	2.3	3.1

BA – Binding Affinity in kcal/mol; Res – Residue; D(H-A) - Distance between hydrogen and acceptor atom in Å; D(D-A) - Distance between donor and acceptor atom in Å

CONCLUSION

This research presents a comprehensive investigation into the structural, spectral, and electronic properties of two novel compounds, 4TFMPIC and 4TFMPTU, utilizing Density Functional Theory (DFT) calculations and experimental validation. The structural analysis reveals optimized bond distances and angles, aligning closely with prior experimental data, confirming molecular integrity and stability. Key findings include bond distances within the thiourea and isothiocyanate systems, such as C12=N5 (1.41 Å) and C5-N4 (1.39 Å), with bond angles ranging from 111° to 178°.

Intramolecular hydrogen bonding and C=S groups in 4TFMPTU highlight potential reactivity sites. Spectral studies employ infrared (IR) and ultraviolet (UV) techniques. IR spectra validate functional group vibrations, such as C-H stretching (3200 cm^{-1}) and C-N stretching (1305 cm^{-1}) in 4TFMPIC, while 4TFMPTU exhibits N-H stretching vibrations at 3558 cm^{-1} and 3680 cm^{-1}. UV analysis shows absorption peaks at 252 nm for 4TFMPIC and 378 nm for 4TFMPTU, corresponding to $n \rightarrow \pi^*$ and $\pi \rightarrow \pi^*$ transitions, respectively. Thermodynamic analysis predicts favorable stability and energy characteristics, with dipole moments of 1.54 D (4TFMPIC) and 7.28 D (4TFMPTU). Mulliken atomic charge distribution highlights electron density variations, reinforcing the compounds' reactive tendencies. Molecular Electrostatic Potential (MEP) analysis maps charge distributions, identifying electrophilic and nucleophilic regions critical for molecular interactions. Frontier Molecular Orbital (FMO) analysis reveals HOMO-LUMO energy gaps of 5.75 eV for 4TFMPIC and 2.12 eV for 4TFMPTU, indicating higher reactivity in the latter. Global hardness and softness values further emphasize the electronic susceptibility of 4TFMPTU, suggesting its potential as a versatile reactive agent. Nonlinear optical (NLO) studies highlight hyperpolarizability values, with 4TFMPIC demonstrating superior NLO properties ($\beta = 1.511 \times 10^{-30}$ esu), making it a promising material for optical applications. Drug-likeness evaluation, based on Lipinski's and Veber's rules, supports 4TFMPTU as a viable drug candidate due to its molecular weight, hydrogen bond characteristics, and bioavailability. Molecular docking studies reveal strong binding affinities (-5.0 to -6.0 kcal/mol) against protein targets, including cancer-related enzymes and SARS-CoV-2 spike proteins, positioning these compounds for pharmaceutical exploration. Overall, this multi-faceted study integrates theoretical modeling with experimental approaches, providing profound insights into structural stability, electronic behavior, and biological activity. These findings underscore the compounds' potential in materials science, drug discovery, and molecular engineering applications.

References

1. van den Bosch TJM, Tan K, Joachimiak A, Welte CU. Functional profiling and crystal structures of isothiocyanate hydrolases found in gut-associated and plant-pathogenic bacteria. Appl Environ Microbiol. 2018;84:e00478-18.
2. Zhang Y. Allyl isothiocyanate as a cancer chemopreventive phytochemical. Mol Nutr Food Res. 2010;54:127–135.
3. Wu X, Zhou Q, Xu K. Are isothiocyanates potential anti-cancer drugs? Acta Pharmacol Sin. 2009;30:501–512.
4. Dufour V, Stahl M, Baysse C. The antibacterial properties of isothiocyanates. Microbiology. 2015;161:229–243.
5. Dufour V, Stahl M, Rosenfeld E, Stintzi A, Baysse C. Insights into the mode of action of benzyl isothiocyanate on Campylobacter jejuni. Appl Environ Microbiol. 2013;79:6958–6968.
6. Jang HW, et al. Analysis and antioxidant activity of extracts from broccoli (Brassica oleracea L.) sprouts. J Agric Food Chem. 2015;63:1169–1174.

7. Li Y, et al. Sulforaphane, a dietary component of broccoli/broccoli sprouts, inhibits breast cancer stem cells. Clin Cancer Res. 2010;16:2580–2590.
8. Mbithi S, et al. Effects of sprouting on nutrient and antinutrient composition of kidney beans (Phaseolus vulgaris var. Rose coco). Eur Food Res Technol. 2001;212:188–191.
9. Xie SH, et al. DNA damage and oxidative stress in human liver cell L-02 caused by surface water extracts during drinking water treatment in a waterworks in China. Environ Mol Mutagen. 2010;51:229–235.
10. Podsedek A. Natural antioxidants and antioxidant capacity of Brassica vegetables: A review. Food Sci Technol. 2007;40:1–11.
11. Prawan A, et al. Structural influence of isothiocyanates on the antioxidant response element (ARE)-mediated heme oxygenase-1 (HO-1) expression. Pharm Res. 2008;25:836–844.
12. Hasija A, Thompson AJ, Singh L, S N M, Mangalampalli KSRN, McMurtrie JC, Bhattacharjee M, Clegg JK, Chopra D. Plastic deformation in a molecular crystal enables a piezoresistive response. Small. 2023;19(12):e2206169.
13. Qiao L, Zhang Y, Hu W, Guo J, Cao W, et al. Synthesis, structural characterization and quantum chemical calculations on 1-(isomeric methylbenzoyl)-3-(4-trifluoromethylphenyl)thioureas. J Mol Struct. 2017;1141:309–321.
14. Rodriguez-Fernandez E, Manzano JL, Benito JJ, Hermosa R, Monte E, Criado JJ. Thiourea, trizole and thiadiazine compounds and their metal complexes as antifungal agents. J Inorg Biochem. 2005;99:1558–1572.
15. Faizi MSH, et al. Crystal structure, Hirshfeld surface analysis and DFT studies of 4-methyl-2-({[4-(trifluoromethyl)phenyl]imino}methyl)phenol. Acta Crystallogr E. 2020;76(8):1325–1330.
16. Kumar B, et al. Crystallographic structure analysis of 4-phenoxy-2-(4-(trifluoromethyl)phenyl) quinazoline. AIP Conf Proc. 2018;2006:030015.
17. Dahinel I, et al. Acridin-9-yl isothiocyanate: Comparison of structural parameters from quantum chemical calculations with corresponding X-ray data. Chem Pap. 2001;55(2):113–117.
18. Rahman FU, et al. Thiourea derivatives, simple in structure but efficient enzyme inhibitors and mercury sensors. Molecules. 2021;26(15):4506.
19. Javadzade T, et al. Synthesis, structural analysis, DFT study, antioxidant activity of metal complexes of N-substituted thiourea. 2023;231:116274.
20. Balachandran V, Murali MK. FT-IR and FT-Raman spectral analysis of 3-trifluoromethyl phenyl isothiocyanate. Vib Spectrosc. 2011;40:5105–5107.
21. Silverstein M, Basseler GC, Morill C. Spectrometric identification of

organic compounds. New York: Wiley; 1981.
22. Beg MAA, Clark HC. Chemistry of the trifluoromethyl group. Can J Chem. 1962;40:393–398.
23. Clark RJH, Williams CS. Infra-red spectra (3000-200 cm-1) of metal isothiocyanate complexes. Spectrochim Acta. 1966;22(6):1081–1090.
24. Rao CNR. Contribution to the infrared spectra of organosulphur compounds. Can J Chem. 1964;42:36–42.
25. Ravi B, Jegatheesan A, et al. Optical and conductivity analysis of thiourea single crystals. Rasayan J Chem. 2014;7(3):287–294.
26. Trivedi MK, et al. An impact of biofield treatment on spectroscopic characterization of pharmaceutical compounds. Mod Chem Appl. 2015;3(3):159.
27. Madhurambal G, et al. Thermal, UV and FTIR spectral studies of urea-thiourea zinc chloride single crystal. J Therm Anal Calorim. 2010;100:763–768.
28. Ravi B, Jegatheesan A, et al. Optical and conductivity analysis of thiourea single crystals. Rasayan J Chem. 2014;7(3):287–294.
29. Raveendiran C, Prabukanthan P, Madhavan J, Vivekanand PA, Arumugam N, Almansour AI, Kumar RS, Alaqeel SI, Perumal K. Synthetic pathway of 2-fluoro-N,N-diphenylbenzamide with opto-electrical properties: NMR, FT-IR, UV-Vis spectroscopic, and DFT computational studies of the first-order nonlinear optical organic single crystal. Green Process Synth. 2023;11(1):1148–1162.
30. Srinivasan S, Gunasekaran S, Ponnambalam U, Savarianandam A, Gnanaprakasam S, Natarajan S. Indian J Pure Appl Phys. 2005;43:459.
31. Khadom AA, Kadhim MM, Anaee RA, Mahood HB, Mahdi MS, Salman AW. Theoretical evaluation of Citrus Aurantium leaf extract as green inhibitor for chemical and biological corrosion of mild steel in acidic solution: statistical, molecular dynamics, docking, and quantum mechanics study. J Mol Liq. 2021;343:116978.
32. Khadom AA, Kadhim MM, Anaee RA, Mahood HB, Mahdi MS, Salman AW. Theoretical evaluation of Citrus Aurantium leaf extract as green inhibitor for chemical and biological corrosion of mild steel in acidic solution: statistical, molecular dynamics, docking, and quantum mechanics study. J Mol Liq. 2021;343:116978.
33. Bine F, Tasheh S, Nkungli N. Corrosion inhibition of aluminium in gas and acid media by some chalcone-based N-(3-aminopropyl)imidazoles: TD-DFT-based FMO, conceptual DFT, QTAIM and EDA studies. Comput Chem. 2021;9:37–63.
34. Cao M, Gao A, Liu Y, Zhou Y, Sun Z, Li Y, He F, Li L, Mo L, Liu R, et al. Theoretical study on electronic structural properties of catalytically reactive metalloporphyrin intermediates. Catalysts. 2020;10:224.
35. Karabacak M, Sinha L, Prasad O, Cinar Z, Cinar M. The spectroscopic (FT-Raman, FT-IR, UV and NMR), molecular electrostatic potential, polarizability and hyperpolarizability, NBO and HOMO–LUMO

analysis of monomeric and dimeric structures of 4-chloro-3,5-dinitrobenzoic acid. Spectrochim Acta A. 2012;93:33–46.

36. Abchir O, Daoui O, Nour H, Yamari I, Elkhattabi S, Errougui A, Chtita S. Cannabis constituents as potential candidates for alpha-amylase inhibitor. Sci Afr. 2023;21:e01745.
37. Mahal A, Al-Janabi M, et al. Molecular docking, drug-likeness and DFT study of some modified tetrahydrocurcumins as potential anticancer agents. Saudi Pharm J. 2024;32:101889.
38. Fukunishi Y, Kurosawa T, Mikami Y, Nakamura H. Prediction of synthetic accessibility based on commercially available compound databases. J Chem Inf Model. 2014;54(12):3259–3267.

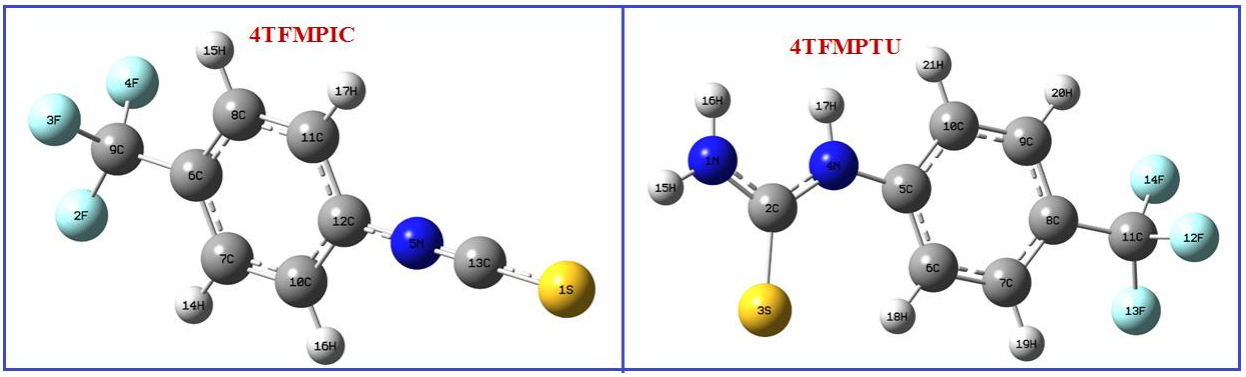

Fig. 1 Optimized structure of the title compounds

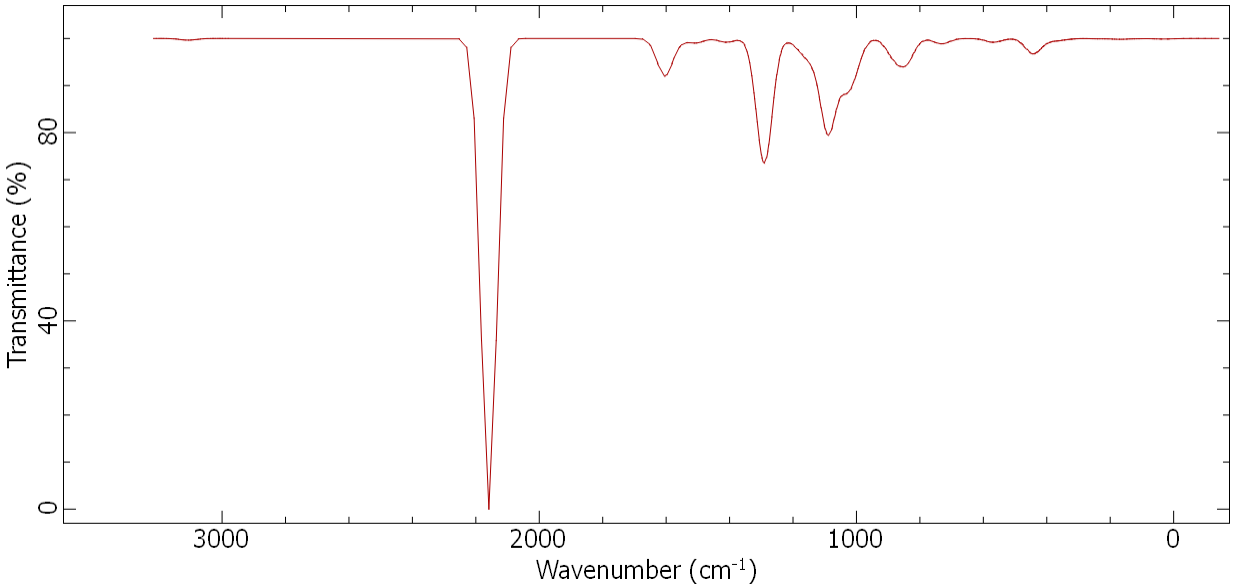

Fig. 2 Theoretically Computed IR Spectra of 4TFMPIC

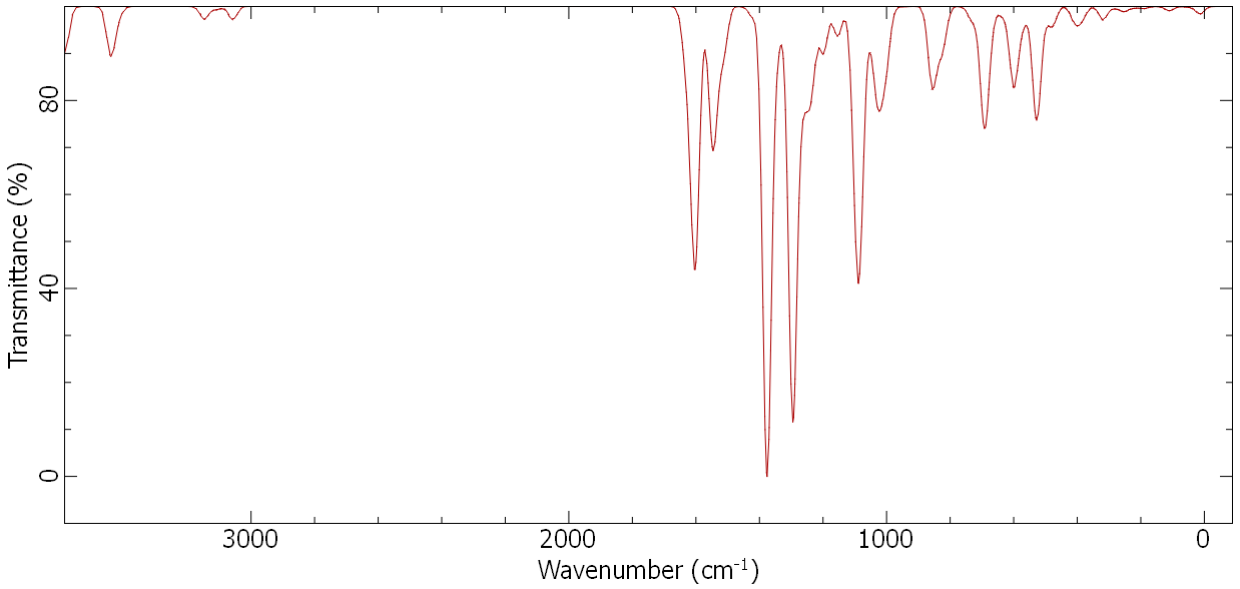

Fig. 3 Theoretically Computed IR Spectra of 4TFMPTU

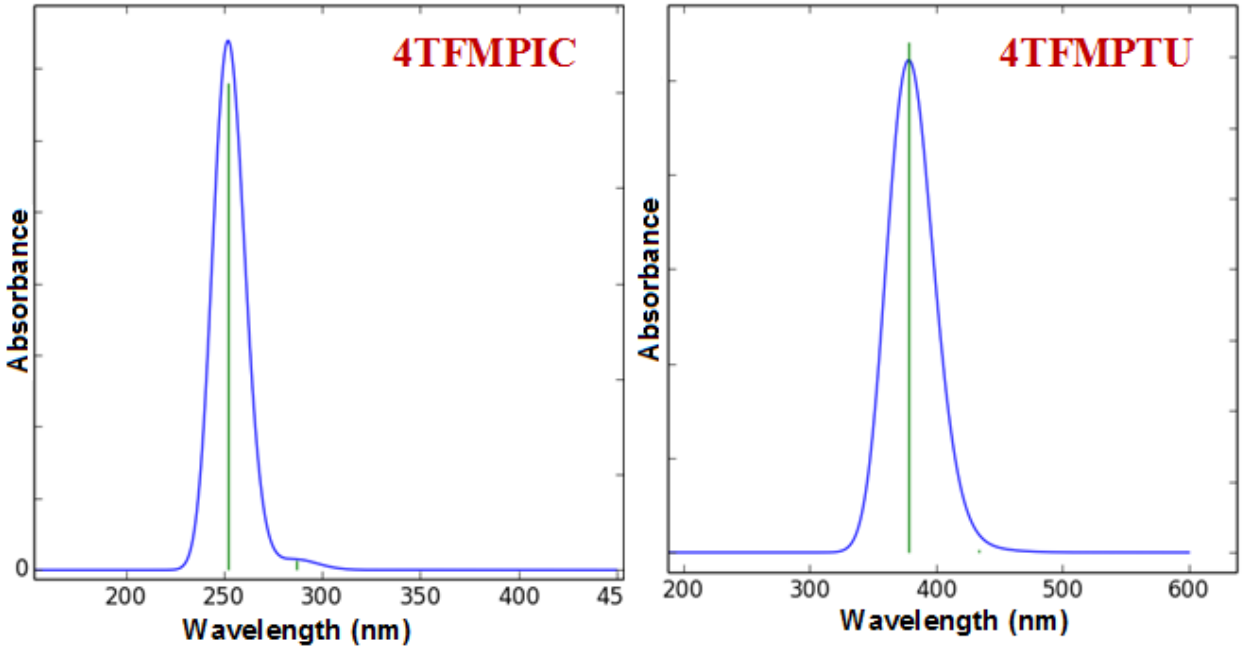

Fig. 4 Theoretical UV spectra for 4TFMPIC and 4TFMPTU

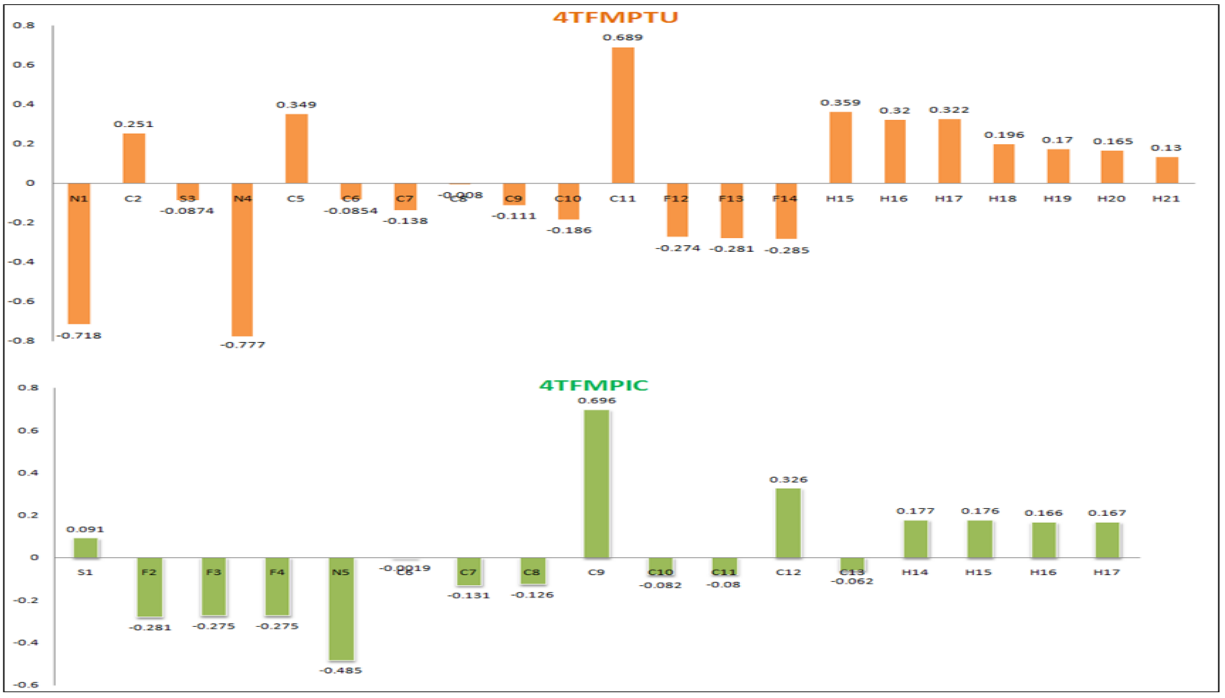

Fig. 5 Graphical representation of Mulliken atomic charges of title compounds

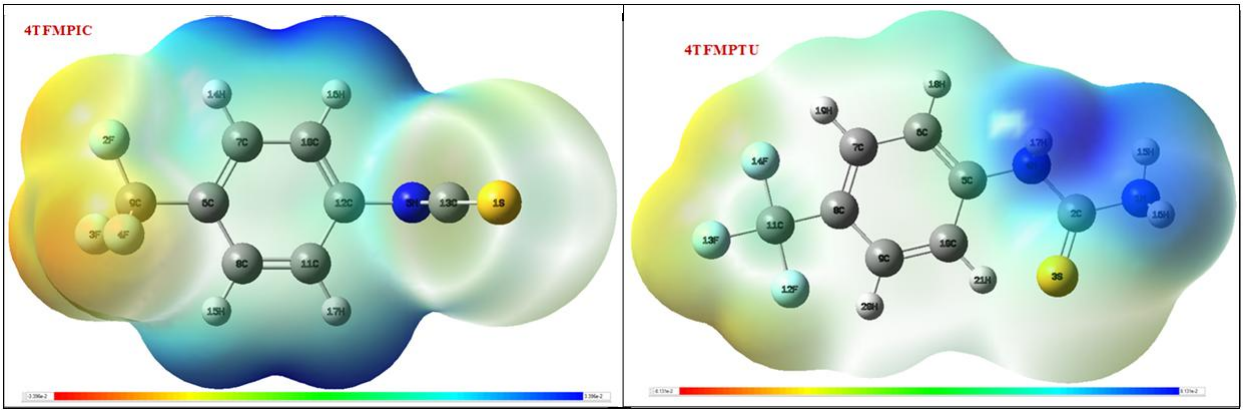

Fig. 6 The electrostatic potential map (3D) of title compounds

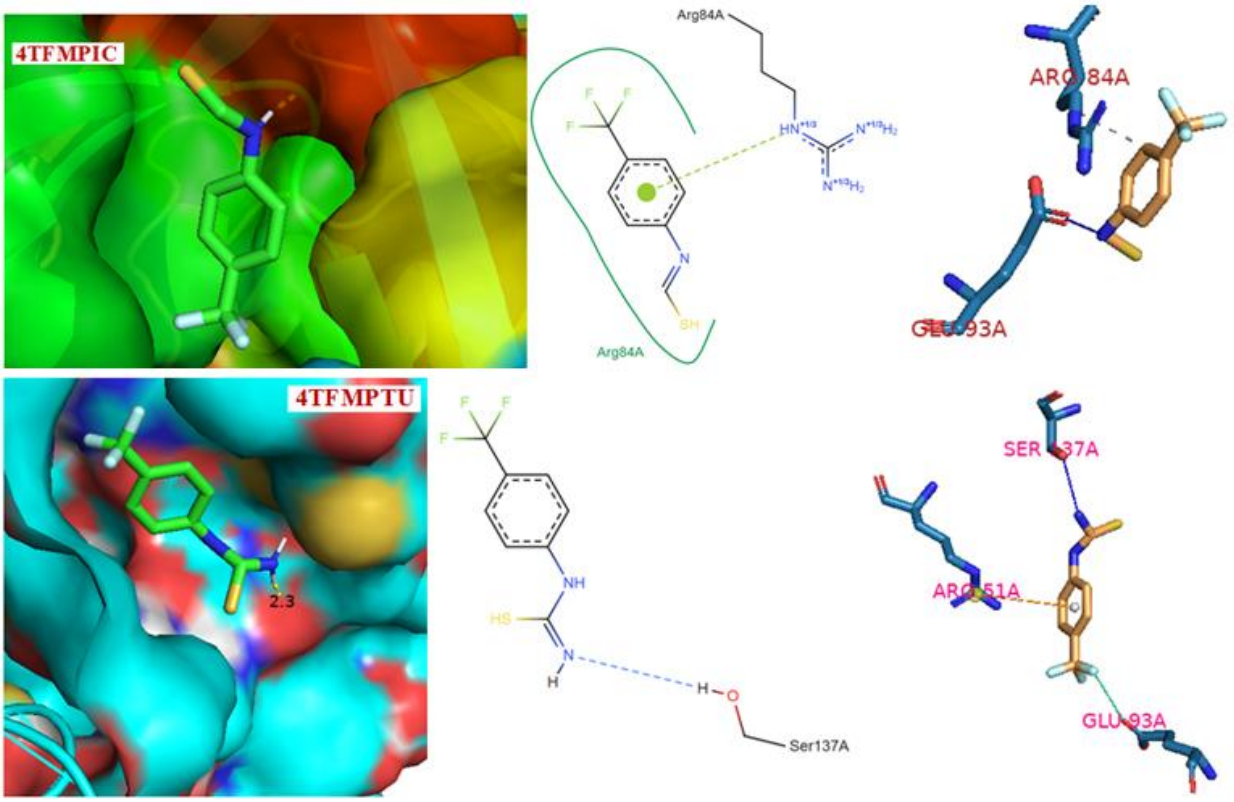

Figures 7. 2D and 3D views of the interactions of title compounds with protein 5NQR

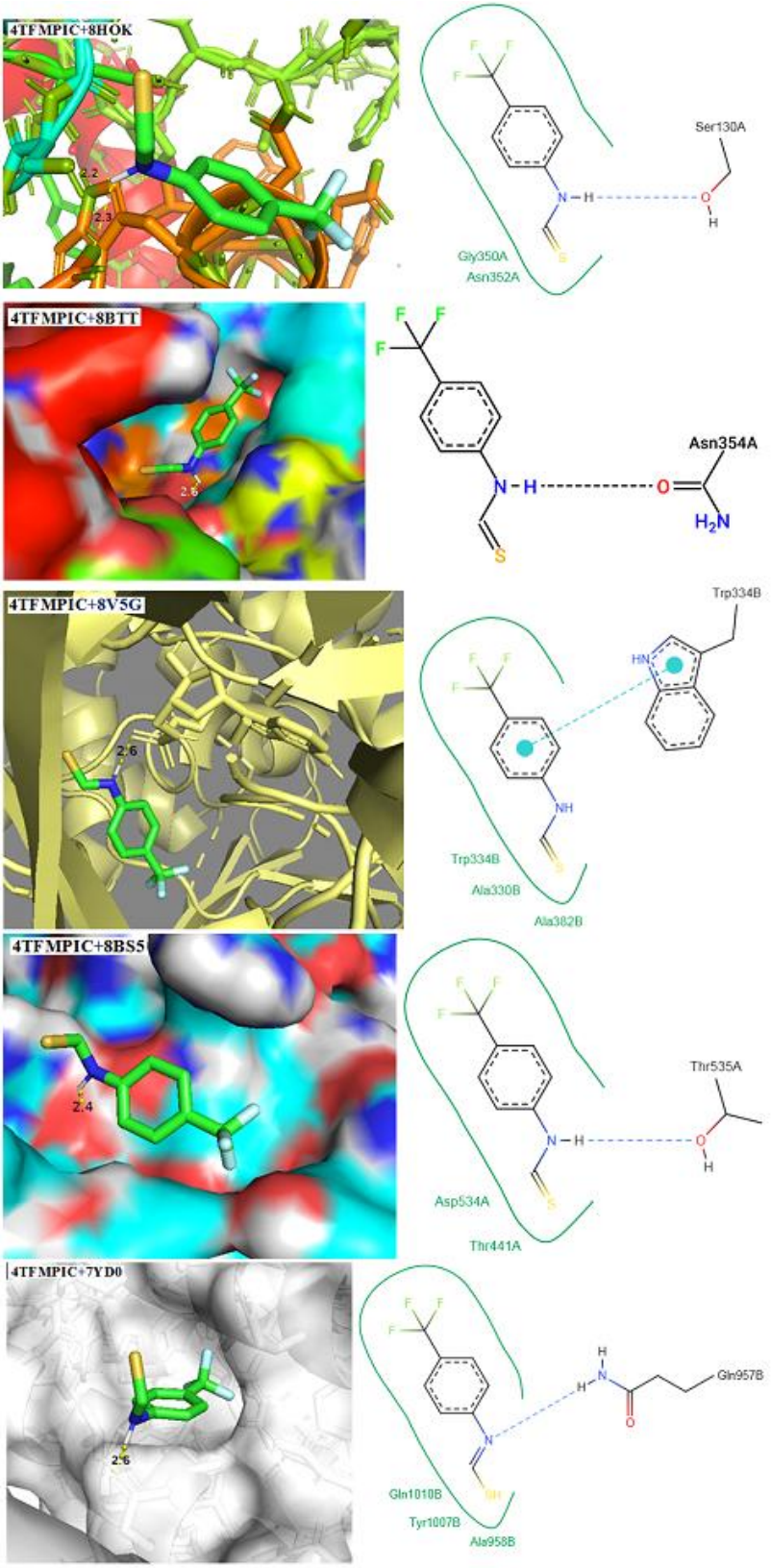

Fig 8a. The binding interactions with five proteins and 2D pose view of 4TFMPIC

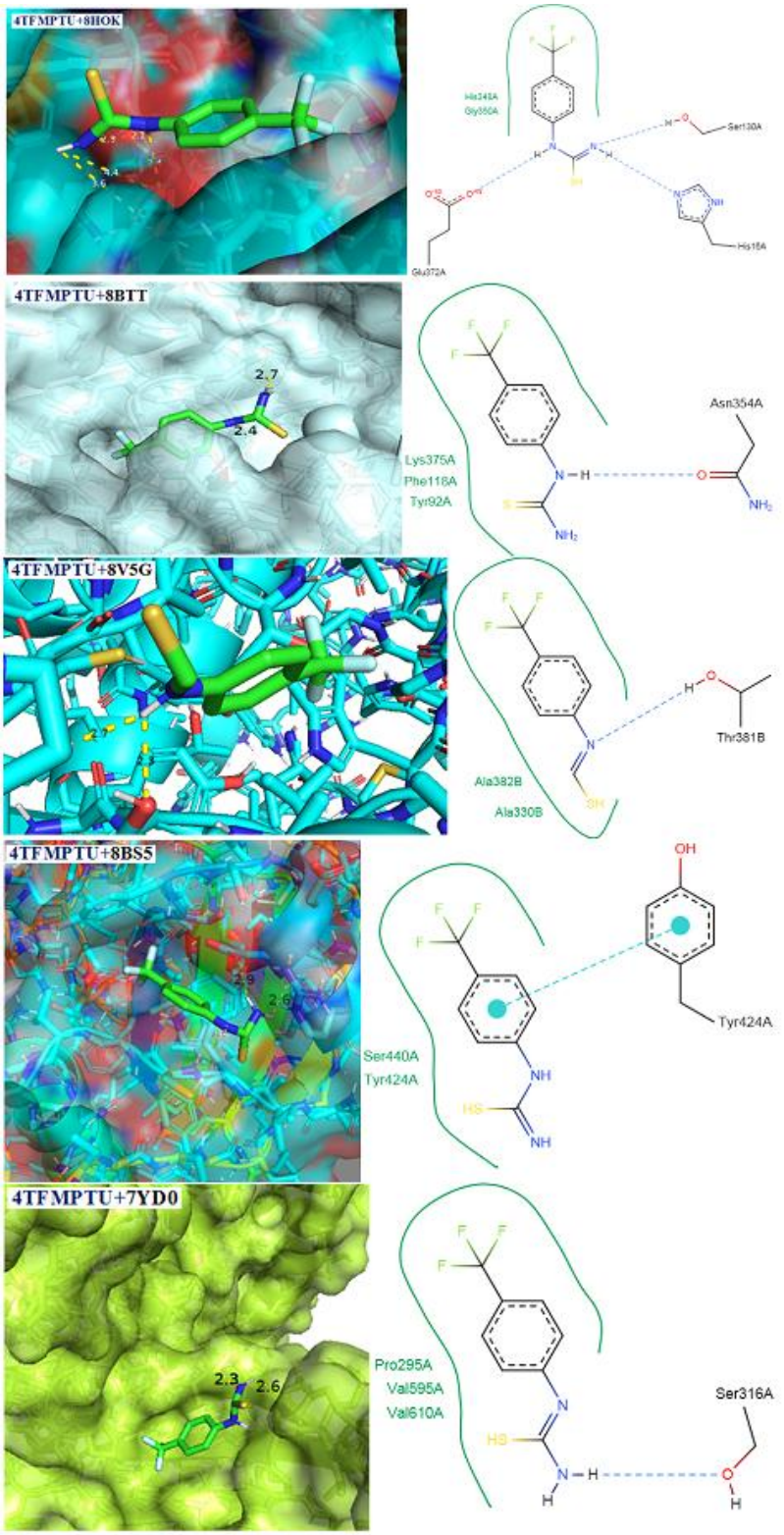

Fig 8b. The binding interactions with five proteins and 2D pose view of 4TFMPTU